Real-Time Monitoring of the Stable Free Radical Polymerization of Styrene via in-Situ Mid-Infrared Spectroscopy

Anthony J. Pasquale and Timothy E. Long*

Department of Chemistry, Virginia Polytechnic Institute and State University, Blacksburg, Virginia 24061-0212

Received July 27, 1999

Introduction. Controlled polymerization routes permit the synthesis of well-defined macromolecules with controlled chemical composition, predictable molecular weight, and narrow molecular weight distribution.[1] The ability to control polymer architecture is essential in advanced technological applications where well-defined macromolecular architectures are required. Control of chain-growth polymer architecture has been traditionally achieved using living anionic,[2,3] cationic,[4] or group-transfer[5] polymerization procedures. Synthetic methodologies for controlled polymerization have been expanded with recent developments in both stable free radical polymerization (SFRP)[6] and atom transfer radical polymerization (ATRP).[7]

On the basis of the earlier work of Rizzardo et al.[8] in nitroxide-mediated stable free radical polymerization, Georges et al.[9] first reported the preparation of polystyrene with low polydispersity using bulk free radical polymerization of styrene initiated by a conventional free radical initiator, benzoyl peroxide (BPO), in the presence of the stable nitroxide free radical, 2,2,6,6-tetramethyl-1-piperidinyloxy (TEMPO) at 125 °C. The SFRP process involves a desirable equilibrium between nitroxide-capped polymer chains and uncapped polymer radicals. The uncapped polymer radicals are then able to chain extend via styrene monomer addition (Scheme 1). The success of this method arises from the unique feature that the nitroxide radicals will react with carbon radicals at near diffusion-controlled rates but will not react with other oxygen-centered radicals or initiate additional polymer chains.

An indication of the controlled nature of the SFRP of styrene is typically accomplished by the demonstration of a linear increase in molecular weight with conversion.[9,10] Kinetic information is commonly obtained by withdrawing samples and analyzing for residual monomer with gravimetric and chromatographic methods.[11] In addition, more sophisticated analytical methods have recently been applied to study SFRP kinetics. For example, Georges et al. have utilized in-situ ESR spectroscopy to study the SFRP process,[11−15] and Hawker et al. have recently applied ^{1}H NMR to evaluate initiator efficiency for SFRP processes using deuterated styrene.[16]

In-situ mid-infrared spectroscopy is a state-of-the-art, real-time, monitoring technique that is well-suited to obtain real-time structural and kinetic information on controlled polymerization processes such as SFRP.[17] In addition, reactions are analyzed without complicated reactor modifications or expensive deuterated monomers. Previously, Long et al.[18] have utilized in-situ near-infrared (NIR) (10 000−4000 cm $^{-1}$) spectroscopy using fiber-optic probe technology to obtain solution polymerization kinetics of living anionic processes. More recently, Puskas et al.[19,20] and Storey et al.[21] have reported the application of in-situ mid-infrared (4000−650 cm^{-1}) spectroscopy to monitor living cationic polymerization processes. In addition, Bradley and Long recently applied in-situ mid-infrared spectroscopy to study melt-phase acidolysis and ester-exchange polymerization mechanisms.[22] These previous efforts have demonstrated the versatility of in-situ infrared spectroscopy, and we report herein the application of this instrumentation to monitor the stable free radical polymerization of styrene.

Scheme 1

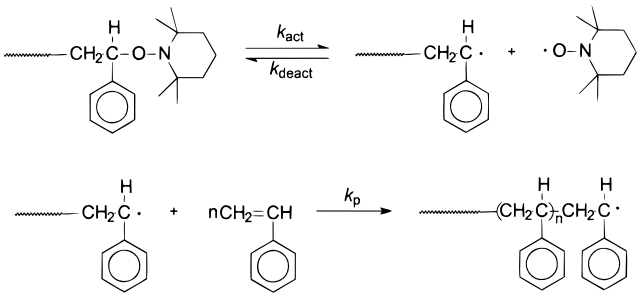

Results and Discussion. In-situ mid-infrared spectroscopy was utilized to monitor the bulk SFRP reaction of styrene (Aldrich, vacuum-distilled from calcium hydride) initiated by BPO (Aldrich, used as received) in the presence of TEMPO (Aldrich, used as received). A ReactIR 1000 (ASI Applied Systems) reaction analysis system equipped with a light conduit and DiComp (diamond composite) insertion probe was used to collect mid-FTIR spectra of the polymerization reaction. The details and capabilities of the ReactIR 1000 based on attenuated total reflectance (ATR) have been described in detail previously.[21] An example procedure for the polymerization at 132 °C is as follows. The reaction was carried out in a 100 mL, round-bottomed, two-necked flask that was fitted with the DiComp probe. To the flask was added a magnetic stir bar, 35 mL of styrene (350 mmol), and 0.368 g of TEMPO (2.36 mmol). Although a magnetic stir bar did not provide adequate agitation at higher conversions due to the extremely high bulk viscosity, it facilitated the intimate contact of the reaction mixture with the probe tip and reduced the likelihood of spurious oxygen ingress. The flask was sealed under nitrogen with a rubber septum, and a thermocouple was inserted through the septum to simultaneously monitor the temperature of the reaction mixture. The ReactIR 1000 was programmed to collect spectra every minute for the first 90 min and then every 5 min for the remaining 24 h. An oil bath at 142 °C was raised to the reaction flask, and IR data acquisition was initiated. After several minutes the temperature of the styrene/TEMPO solution in the reaction flask stabilized at 132 °C. (The large temperature difference between the oil bath and reaction mixture is speculated to be due to the heat loss due to the stainless steel DiComp probe.) Infrared analysis indicated that the styrene/TEMPO solution was stable in the absence of benzoyl peroxide, and appreciable thermal polymerization was not observed during this short period. After the temperature of the reaction stabilized at 132 °C, a solution of 0.440 g of BPO (1.818 mmol) dissolved in 5 mL of styrene was added via syringe. After 14 h the viscosity of the reaction increased dramatically, and stirring

10.1021/ma9912498 CCC: $18.00
Published on Web 10/21/1999

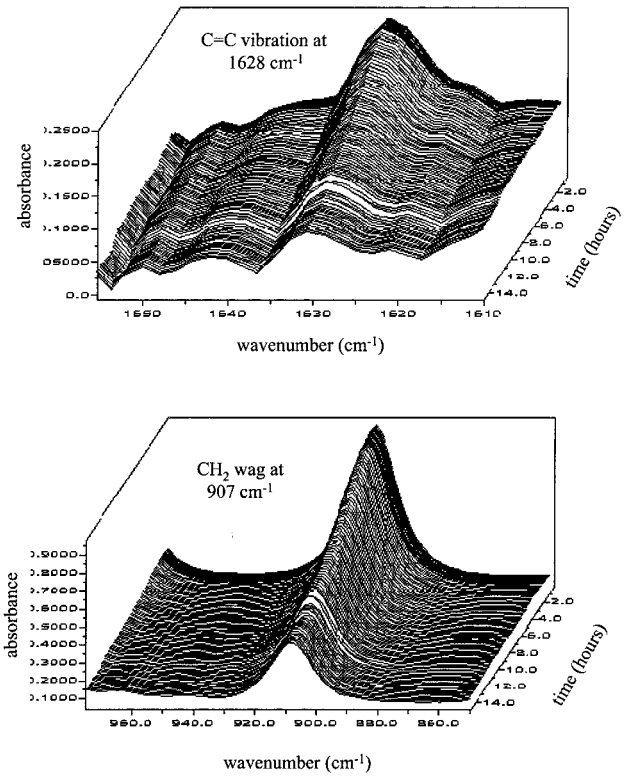

Figure 1. Real-time FTIR "molecular videos" of styrene monomer: C═C stretch at 1628 cm^{-1} (top) and ═CH_2 wag at 907 cm^{-1} (bottom).

stopped due to the high bulk viscosity. Additionally, the infrared absorbances associated with the styrene monomer stabilized and stopped decreasing. The polymer product was cooled to room temperature, dissolved in chloroform, precipitated into methanol, and dried overnight under vacuum to yield 30.54 g (84% conversion) of TEMPO-terminated polystyrene of $M_n = 20\,600$ ($M_w/M_n = 1.04$) determined by size exclusion chromatography (Waters GPC with external 410 RI detector and Viscotek 150R viscometer, NMP/P_2O_5 (0.02 M) solvent at 60 °C and 1.0 mL/min flow rate). Styrene polymerization at 126 °C yielded 26.6 g (73.2% conversion) of TEMPO-terminated polystyrene of $M_n = 18\,000$ ($M_w/M_n = 1.04$) after a reaction time of 16 h. NMR analysis of the vacuum-dried TEMPO-terminated polystyrenes indicated the absence of appreciable residual monomer and/or precipitation solvent. The reproducibly low molecular weight distributions were indicative that the presence of the probe did not deleteriously affect the controlled polymerization process. To eliminate concerns associated with the polymer isolation process, samples were directly removed from the reaction mixture, dried to a constant weight, and analyzed using size exclusion chromatography. In all cases, the molecular weight distributions obtained using the NMP/P_2O_5 (0.02 M) solvent system exhibited M_w/M_n values ranging from 1.04 to 1.09.

Styrene monomer exhibited two strong infrared absorbances that were easily monitored. The ReactIR 1000 with light conduit technology allowed for the generation of real-time mid-IR spectra from 4000 to 650 cm^{-1}. The "molecular videos" of the C═C (1628 cm^{-1}) and ═CH_2 (907 cm^{-1}) absorbances for styrene polymerization at 132 °C are shown in Figure 1. Both monomer and polymer infrared absorbances were analyzed to produce a symmetrical X-shaped plot, which is characteristic of

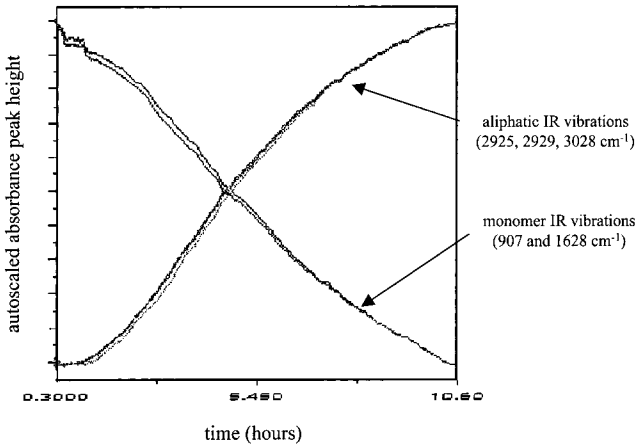

Figure 2. Real-time profiles of increasing alkyl C−H polymer peak heights (2925, 2929, and 3028 cm^{-1}) and decreasing vinyl monomer peak heights (907 and 1628 cm^{-1}).

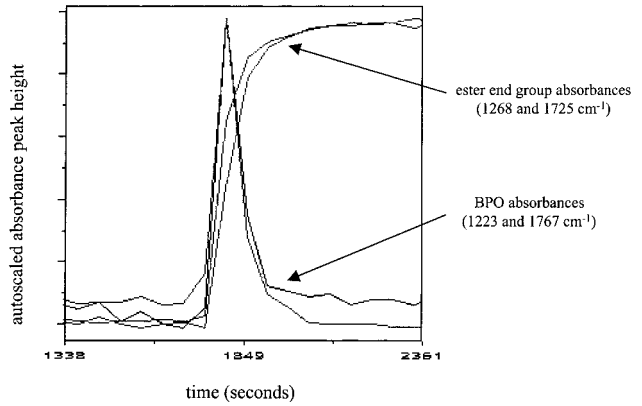

Figure 3. Real-time profiles of BPO (C═O at 1767 cm^{-1} and C−O−C at 1223 cm^{-1}) and polymer ester end group (C═O at 1725 cm^{-1} and C−O−C at 1268 cm^{-1}).

a controlled polymerization process such as SFRP. The X-plot produced from three alkyl C−H absorbances (2925, 2929, and 3028 cm^{-1}), exhibited by the forming polymer, and the two vinyl absorbances (907 and 1628 cm^{-1}), exhibited by the disappearing monomer, for the polymerization at 132 °C is shown in Figure 2. The absorbance peak height (*y*-axis) was autoscaled so that the relative changes in each of the monitored absorbances were directly comparable. As one can see, the profiles for the three polymer alkyl absorbances as well as the two monomer vinyl absorbances overlap and agree favorably with each other as expected for a controlled polymerization process.

To demonstrate the sensitivity of this technique, the initiation step of the polymerization was monitored by profiling the initiator, BPO, as well as the ester end group that is formed from addition of the initiating radical to one styrene monomer. The profiles of two BPO absorbances, C═O (1767 cm^{-1}) and C−O−C (1223 cm^{-1}), were compared with two polymer ester end group absorbances, C═O (1725 cm^{-1}) and C−O−C (1268 cm^{-1}), and are shown in Figure 3. The absorbance peak heights (*y*-axis) were again autoscaled to allow for visual comparison. After an elapsed time of 29 min and 9 s of data collection, the BPO/styrene solution was added to the TEMPO/styrene solution at 132 °C. The BPO absorbances appeared after addition of the BPO to the reaction and then rapidly decayed completely. From the profile of BPO decay, the half-life of BPO in the presence of styrene and TEMPO at 132 °C was estimated to be

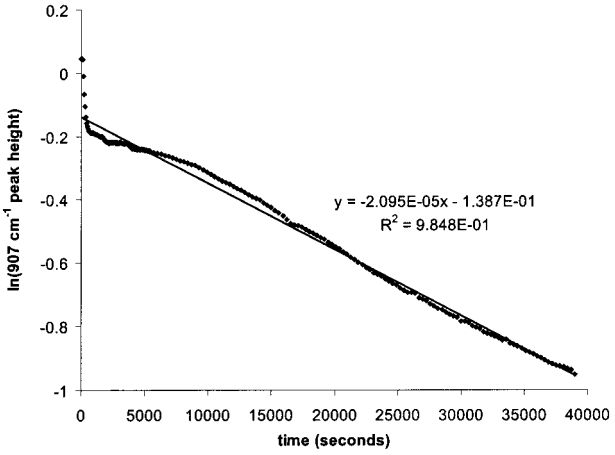

Figure 4. First-order kinetic plot for styrene SFRP polymerization at 132 °C (determined from the real-time FTIR profile of the styrene $=CH_2$ absorbance (907 cm^{-1})).

approximately 50 s. In addition, during the same time period as the BPO decay, the formation of the ester polymer end groups was observed as the initiating radicals added to styrene monomer. The ester end group absorbances at 1725 and 1268 cm^{-1} increased upon BPO addition and leveled upon complete consumption of BPO. Efforts continue to also identify and follow an absorbance associated with the formation of the nitroxide chain end.

Apparent rate constants were also determined from the real-time decay profiles of the styrene monomer. Figure 4 depicts the first-order kinetic plot constructed from the real-time profile for the decay of the $=CH_2$ absorbance (907 cm^{-1}) of the styrene monomer for the polymerization at 132 °C. As stated earlier, data points were collected every minute for the first 90 min and then every 5 min for the remainder of the reaction. The initial steep decrease in the absorbance seen in Figure 4 is due to the increasing temperature of the reaction mixture since BPO was not added until constant temperature and constant $=CH_2$ absorbance were observed. Once the reactor temperature stabilized, BPO was added to the reactor, and the monomer $=CH_2$ absorbance decreased at a constant rate. Data from the real-time profile of the $=CH_2$ absorbance allowed for the calculation of an apparent first-order rate constant from the slope, which is equal to the rate of propagation times the concentration of growing polymer radicals ($k_{app} = k_p[P_n^\bullet]$), assuming no termination or side reactions occur. From the first-order kinetic plot, the apparent rate constant for the reaction was determined to be $(2.09 \pm 0.02) \times 10^{-5}$ s^{-1} at 132 °C and $(1.15 \pm 0.02) \times 10^{-5}$ s^{-1} at 126 °C. It is important to note that the rate constants determined using the $=CH_2$ absorbance (907 cm^{-1}) were in good agreement with the rate constants determined using the C=C absorbance (1628 cm^{-1}). Although a stable baseline was difficult to identify for the lower intensity C=C absorbance at 1628 cm^{-1}, the apparent rate constant at 132 °C was $(1.99 \pm 0.06) \times 10^{-5}$ s^{-1}, which agrees favorably with the value determined using the $=CH_2$ absorbance. Interestingly, it was observed that the slope of the line in Figure 4 was not completely linear over the entire polymerization process. It appeared that the rate of the reaction was slower earlier in the reaction and then increased later. Georges et al. observed a similar phenomenon and developed a *germination efficiency*[11] factor to account for this initial nonlinearity. Additionally, it was observed that at high conversion the rate appeared to decrease. This decrease in rate at higher conversions may be attributed to the increasing solution viscosity and the inability of the magnetic stirrer to eliminate temperature gradients. In addition, propagation rate constants may decrease at high conversions due to radical termination reactions that result in a reduced radical concentration.

Conclusions. Real-time mid-infrared spectroscopy (4000−650 cm^{-1}) monitoring was successfully utilized to follow radical initiation, monomer conversion, and polymer formation during the stable free radical polymerization (SFRP) of styrene initiated by benzoyl peroxide (BPO) in the presence of TEMPO. Apparent rate constants ($k_{app} = k_p[P_n^\bullet]$) were calculated from real-time analysis to be $(2.09 \pm 0.02) \times 10^{-5}$ s^{-1} at 132 °C and $(1.15 \pm 0.02) \times 10^{-5}$ s^{-1} at 126 °C from the profile of the decaying absorbance of the monomer $=CH_2$ wag at 907 cm^{-1}. The half-life of BPO at 132 °C in the presence of styrene and TEMPO was also determined from real-time analysis to be approximately 50 s. The initial results reported herein demonstrate the utility and application for this real-time analytical technique to provide mechanistic and kinetic information for polymerization reactions. Furthermore, the ability to detect the initiator decay and formation of ester end groups demonstrates the sensitivity of the technique and the potential for the study of inter- and-intramolecular interactions as well as side reactions. Future studies will focus on the further development and application of in-situ mid-IR spectroscopy to elucidate polymerization mechanisms, kinetics, sequence distributions, and deleterious side reactions associated with conventional free radical polymerization, SFRP, and anionic solution polymerization processes.

Acknowledgment. Financial support provided by the National Science Foundation (NSF CRIF 9974632), Jeffress Memorial Trust, and the Virginia Tech NSF Science & Technology Center is gratefully acknowledged. The authors also thank Dr. Jennifer Andrews of ASI Applied Systems for many insightful discussions.

References and Notes

(1) Webster, O. W. *Science* **1991**, *251*, 887.
(2) Szwarc, M. *Nature* **1956**, *178*, 1168.
(3) McGrath, J. E. In *Anionic Polymerization: Kinetics, Mechanisms, and Synthesis*; ACS Symposium Series 166; American Chemical Society: Washington, DC, 1981.
(4) Matyjaszewski, K. *Cationic Polymerizations: Mechanisms, Synthesis and Applications*; Marcel Deker: New York, 1996.
(5) Sogah, D. Y.; Hertler, W. R.; Webster, O. W.; Cohen, G. M. *Macromolecules* **1987**, *20*, 1473.
(6) Hawker, C. J. *Acc. Chem. Res.* **1997**, *30*, 373.
(7) Patten, T. E.; Matyjaszewki, K. *Adv. Mater.* **1998**, *10*, 901.
(8) Moad, G.; Rizzardo, E.; Solomon, D. H. *Macromolecules* **1982**, *15*, 909.
(9) Georges, M. K.; Veregin, R. P. N.; Kazmaier, P. M.; Hamer, G. K. *Macromolecules* **1993**, *26*, 2987.
(10) Hawker, C. J. *J. Am. Chem. Soc.* **1994**, *116*, 11185.
(11) Veregin, R. P. N.; Odell, P. G.; Michalak, L. M.; Georges, M. K. *Macromolecules* **1996**, *29*, 2746.
(12) Veregin, R. P. N.; Georges, M. K.; Kazmaier, P. M.; Hamer, G. K. *Macromolecules* **1993**, *26*, 5316.
(13) Veregin, R. P. N.; Odell, P. G.; Michalak, L. M.; Georges, M. K. *Macromolecules* **1996**, *29*, 4161.
(14) MacLeod, P. J.; Veregin, R. P. N.; Odell, P. G.; Georges, M. K. *Macromolecules* **1998**, *31*, 530.
(15) Moffat, K. A.; Hamer, G. K.; Georges, M. K. *Macromolecules* **1999**, *32*, 1004.
(16) Hawker, C. J.; Barclay, G. G.; Orellana, A.; Dao, J.; Devonport, W. *Macromolecules* **1996**, *29*, 5245.

(17) Chang, S. Y.; Wang, N. S. In *Multidimensional Spectroscopy of Polymers*; ACS Symposium Series 598; American Chemical Society: Washington, DC, 1995.
(18) Long, T. E.; Liu, H. Y.; Schell, D. M.; Teegarden, D. M.; Uerz, D. S. *Macromolecules* **1993**, *26*, 6237.
(19) Puskas, J. E.; Lanzendörfer, M. G.; Pattern, W. E. *Polym. Bull.* **1998**, *40*, 55.
(20) Puskas, J. E.; Lanzendörfer, M. G. *Macromolecules* **1998**, *31*, 8684.
(21) Storey, R. F.; Donnalley, A. B.; Maggio, T. L. *Macromolecules* **1998**, *31*, 1523.
(22) Bradley, J. R.; Long, T. E. *Polym. Prepr.* **1999**, *40* (1), 564.

MA9912498